Quaternary Geochronology 30 (2015) 524–528

Contents lists available at ScienceDirect

Quaternary Geochronology

journal homepage: www.elsevier.com/locate/quageo

Research paper

Coupled ESR and U-series dating of early Pleistocene *Gigantopithecus* faunas at Mohui and Sanhe Caves, Guangxi, southern China

Qingfeng Shao [a, *], Jean-Jacques Bahain [b], Wei Wang [c], Min Zhu [d], Pierre Voinchet [b], Min Lin [e], Eric Douville [f]

[a] College of Geography Science, Nanjing Normal University, Nanjing 210023, China
[b] CNRS-Muséum National d'Histoire Naturelle, UMR 7209, Paris 75013, France
[c] Guangxi Museum of Nationalities, Nanning 530028, China
[d] Key Laboratory of Vertebrate Evolution and Human Origins of Chinese Academy of Sciences, Institute of Vertebrate Paleontology and Paleoanthropology, Beijing 100044, China
[e] National Key Laboratory of Metrology and Calibration Technology, China Institute of Atomic Energy, Beijing 102413, China
[f] Laboratoire des Sciences du Climat et de l'Environnement, LSCE/IPSL, CNRS-CEA-UVSQ, Domaine du CNRS, Gif/Yvette Cedex 91198, France

ARTICLE INFO

Article history:
Received 22 October 2014
Received in revised form
19 February 2015
Accepted 21 April 2015
Available online 23 April 2015

Keywords:
Coupled ESR/U-series dating
Gigantopithecus fauna
Mohui Cave
Sanhe Cave

ABSTRACT

Several caves of the Guangxi Zhuang Autonomous Region, southern China, have delivered *Gigantopithecus blacki* remains, an extinct Pleistocene giant ape, in association with abundant mammalian faunas. To determine their geological ages, fossil teeth from Mohui and Sanhe Caves were dated using the coupled ESR/U-series method. The teeth from Mohui Cave gave age estimates of 1.69 ± 0.22 Ma and 1.29 ± 0.11 Ma. The Sanhe Cave samples had age estimates ranging from 910 ± 200 ka to 600 ± 150 ka with error weighted mean ages of 890 ± 130 ka and 720 ± 90 ka for the layers 5 and 4, respectively. Our results and previous paleomagnetism data place the *Gigantopithecus* fauna at Mohui Cave between Olduvai and Jaramillo subchrons and suggest that it was coeval with Chuifeng, Longgupo and Liucheng assemblages. The Sanhe fauna is younger, of late early Pleistocene age, and can be dated to the period between Jaramillo subchron and B/M boundary.

1. Introduction

Gigantopithecus blacki is an extinct Pleistocene Asian ape characterized by its exceptionally large molars and a massive mandible. This giant ape was adapted to living in a tropical or subtropical forest environment and consuming a variety of plants (Ciochon et al., 1990). To date, more than 15 localities in southern China and northern Vietnam have yielded *G. blacki* remains associated with abundant mammals, hominin fossils and cultural remains (*e.g.*, Huang et al., 1995; Ciochon et al., 1996; Zheng, 2004; Wang et al., 2005). Based on faunal comparisons, these assemblages are generally divided into three temporal evolutionary stages from the early Lower Pleistocene (stage 1) to the end of the Middle Pleistocene (stage 3) (Jin et al., 2009, 2014). But few sites have been dated radiometrically and thus the chronology of the *Gigantopithecus* faunas remains significantly uncertain.

Recently, several new *Gigantopithecus* localities were discovered in the Guangxi Zhuang Autonomous Region (ZAR) of southern China (Fig. 1). In 2012, a program of coupled ESR and U-series dating (also referred to as coupled ESR-^{230}Th/^{234}U dating) for *Gigantopithecus* faunas was started along with faunal, evolutionary, and paleoenvironmental studies (*e.g.*, Wang et al., 2007, 2014a,b,c; Wang, 2009; Jin et al., 2009). Teeth from various Guangxi ZAR caves have been sampled. Among them, teeth from Chuifeng Cave (stage 1) have been dated from 1.97 ± 0.19 Ma to 1.38 ± 0.17 Ma (Shao et al., 2014b). The present paper reports ages for the faunal assemblages at Mohui and Sanhe Caves.

2. Materials and methods

2.1. The sites and samples

Mohui Cave (23°34.89′ N, 107°00.13′ E) is located on the southeast margin of the Bubing Basin, at an elevation of 215 m amsl. In 2002–2008, W. Wang and colleagues excavated this cave, which is ~50 m long, 2–6 m wide and 5–6 m high. The cave infillings are

* Corresponding author.
E-mail address: 09396@njnu.edu.cn (Q. Shao).

http://dx.doi.org/10.1016/j.quageo.2015.04.008
1871-1014/

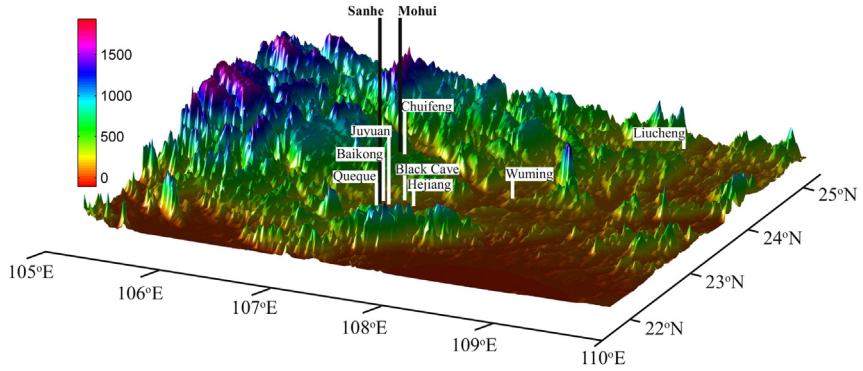

Fig. 1. *Gigantopithecus* localities in Guangxi Zhuang Autonomous Region of southern China.

~6 m thick, which were divided into five layers (Fig. 2A; Wang et al., 2005). The bottom layer (L.1) is made of dark brown fluvial sands, and the top layer (L.5) is formed by gray–white flowstone. In between, the layers (L.2–4) are composed of brown sandy–clay and sandy silt with limestone breccias. Sixteen *G. blacki* teeth, associated with numerous other mammalian fossil teeth and bones, were recovered from the layer 3, which is ~210 cm thick (Wang et al., 2005).

The Mohui faunal assemblage comprises 28 genus/species, including some typical early Pleistocene species of stage 1 (Table S1). Among them, the predominant species are primates (*Macaca* sp. and *G. blacki*), suid (*Sus xiaozhu* and *Sus peii*), porcupine (*Hystrix magna* and *Hystrix kiangsenensis*) and deer (*Muntiacus* sp., *Cervavitus fengqii*, and *Cervavitus yunnanensis*). Two teeth of *Rhinoceros fusuiensis*, MHC-1 and MHC-2, from layer 3 at depths of 110 cm and 170 cm below the datum line, respectively, were analyzed in the present study (Table S2).

Sanhe Cave (22°16.49′ N, 107°30.66′ E), located in the Chongzuo Ecological Park, is a tubular karst cave ~160 m long, ~200 m amsl and ~70 m above the local active river level. C. Jin and colleagues excavated this cave in 2004–2008, and seven layers were identified in ~12 m thick infilling (Fig. 2B; Jin et al., 2009; Wang et al., 2014b). The layer 4, a brownish yellow sand with thin horizons cemented by carbonates, yielded 56 *G. blacki* teeth. A few *G. blacki* teeth occurred from the sandy silts of layer 5.

The Sanhe mammalian assemblage contains 10 orders, 24 families, 64 genera and 84 species, and shows distinct early Pleistocene Oriental tropical fauna characteristics (stage 2) (Jin et al.,

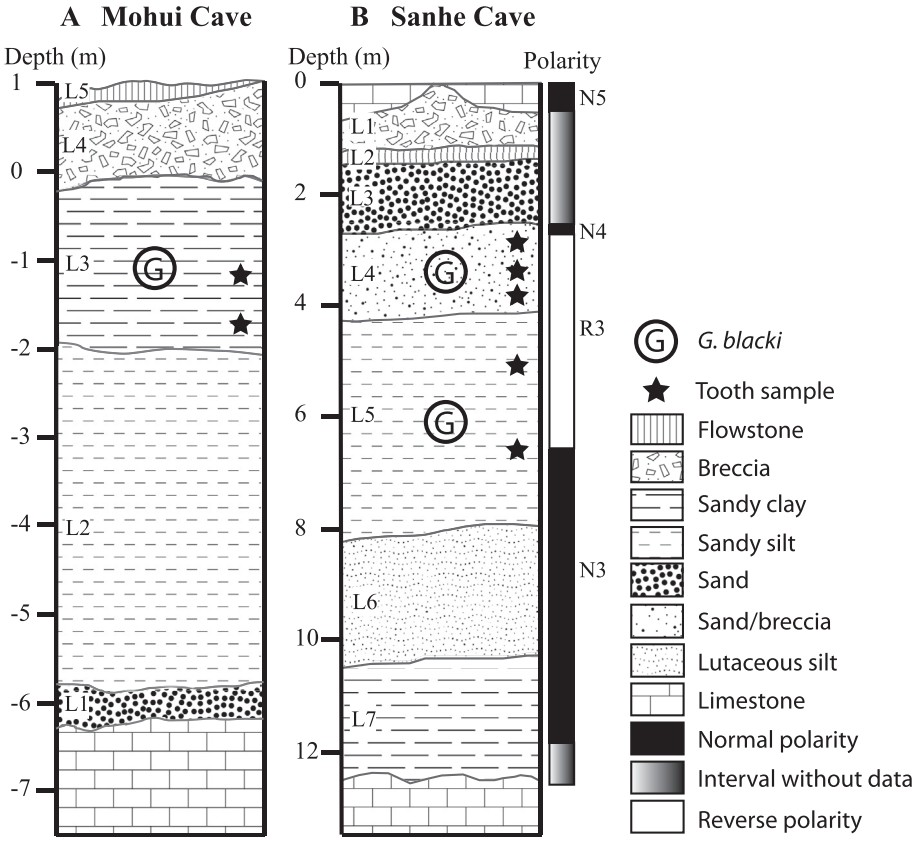

Fig. 2. A) Stratigraphic section of the Mohui Cave, modified according to Wang et al. (2005); B) Stratigraphic and paleomagnetic sequences of the Sanhe Cave, modified according to Jin et al. (2009), Wang et al. (2014b) and Sun et al. (2014). Sample positions represent the depths for Mohui samples and the layers for Sanhe samples.

2009, 2014). Five excavated mammalian teeth were analyzed in this study: two *Bovidae* teeth (SHC-1 and SHC-3) from layer 5, and one Bovidae tooth (SHC-2), one fragment of a *Sinomastodon* tooth (SHC-4) and one *Rhinoceros* tooth (SHC-5) from layer 4 (Table S2). Unfortunately, depths were not available for these samples.

2.2. Experimental

ESR sample preparation followed Wagner et al. (2010). The dental tissues (enamel, dentine and cementum) of each tooth were separated and cleaned using a dentist's drill. After enamel thicknesses were measured with a micrometer, ~50 μm were removed from both sides and the thicknesses were re-measured. The cleaned enamel pieces were then crushed into powder with a mortar and pestle, and the 100–200 μm fraction was separated by sieving. For each sample, ten enamel aliquots (~100 mg each) were irradiated by a calibrated ^{60}Co γ-ray beam using exponentially increasing doses of 0, 430, 610, 940, 1340, 2300, 3630, 5390, 8340 and 12,410 Gy. ESR analysis was performed on a Bruker EMX spectrometer with a GR 4119 HS resonator operated in X-band (10 GHz) at China Institute of Atomic Energy. Enamel ESR signal at $g = 2.0018$ was measured at room temperature with 1 mW microwave power, 12 mT field scan width, 352 mT center field, 100 kHz modulation frequency, 0.1 mT modulation amplitude and a 81.92 ms time constant.

U–Th isotopic analysis of dental samples was performed on a Neptune multiple collector inductively coupled plasma mass spectrometer (MC-ICPMS) in Nanjing Normal University, China. Chemical preparation of the samples was similar to that described by Shao et al. (2011). Dental fragments were weighed (50–150 mg) and dissolved in 6 N HNO_3 in a Teflon vial containing 30 μl of a ^{229}Th–^{233}U–^{236}U spike. The dissolved sample-spike mixture was heated on a hot plate overnight and re-dissolved in 8 N HCl. The solution was then loaded into an anion exchange resin column (Dowex 1 × 8, 100–200 mesh) for U–Th separation. The U fraction was then purified using a UTEVA resin column in 3 N HNO_3, and the Th fraction was subsequently purified using a second anion exchange resin column in 7 N HNO_3. Finally, the solution of U and Th isolates was evaporated to dryness, and the residues dissolved in 0.5 N HNO_3. To perform simultaneous measurements of U and Th isotopes, a small amount of the sample U fraction (20%–50%) was admixed with the Th fraction. Isotopic measurements of ^{229}Th, ^{230}Th, ^{232}Th, ^{233}U, ^{234}U, ^{235}U, ^{236}U and ^{238}U were subsequently performed on the Neptune MC-ICPMS instrument using a standard sample bracketing technique (Goldstein and Stirling, 2003).

The U-series (US) model (Grün et al., 1988) using the *p*-parameter for describing U-uptake histories was used to evaluate ages. However, the measured ^{230}Th/^{234}U ratios (Fig. 3) limit the use of this model. For samples that showing ^{230}Th/^{234}U > 1 in each tissue, their ages were then evaluated by the Accelerating Uptake (AU) model, which describes U-uptake as an accelerating process defined by an initial uptake rate and a rate acceleration, and introduces the n-parameter to describe U-uptake histories (Shao et al., 2012). The age and associated parameters were calculated by Monte Carlo simulation (Shao et al., 2014a) using the same parameters as the DATA program (Grün, 2009), which uses, for example, dose rate conversion factors from Adamiec and Aitken (1998), and α-efficiency (0.13 ± 0.02) from Grün and Katzenberger-Apel (1994). Error weighted mean age follows McLean et al. (2011).

The measured parameters for calculating coupled ESR/U-series age estimates were summarized in Table S3. Water contents were assumed to be 3 ± 1 wt% in enamel and 7 ± 3 wt% in dentine and cementum (Driessens, 1980). The water contents of 15 ± 5 wt% in sediments were evaluated by drying the sediment samples in an oven at 60 °C for two weeks. The radon loss for each dental tissue was evaluated by the measurement of ^{222}Rn/^{230}Th ratio using γ-ray spectrometry. The sedimentary U, Th and K concentrations were measured in laboratory using a γ-ray spectrometry (Tables S3 and S4).

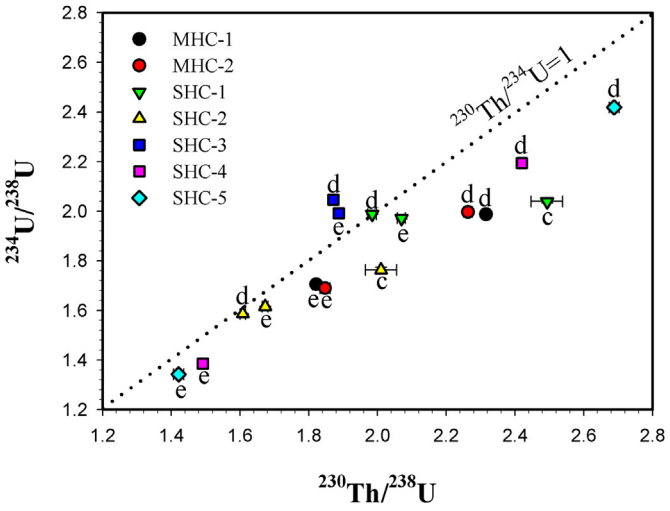

Fig. 3. Plot of activity ratios (^{234}U/^{238}U *vs* ^{230}Th/^{238}U) for samples from Mohui and Sanhe Caves. e: enamel; d: dentine; c: cementum. These data were measured by MC-ICPMS in NNU, China, except for the cementum of SHC-1 and SHC-2, which were measured by ICP-QMS in LSCE, France.

3. Results

The equivalent dose (D_e) was determined from the change in ESR intensity with the irradiation doses, using an exponential saturation plus linear fitting function (E + L) (Berger and Huntley, 1989). For early Pleistocene samples with high paleodoses, the E + L fitting function may produce better dose response curves than commonly used single exponential saturation fitting function (Apers et al., 1981). For Mohui Cave samples, the D_e-values are significantly higher, at 2274 ± 136 Gy for MHC-1 and 2595 ± 138 Gy for MHC-2, than those from Sanhe Cave, which range from 881 ± 54 Gy to 1759 ± 159 Gy (Table S2).

U–Th isotopic analysis was carried out for each dental tissue on mass spectrometry. With respect to U concentration, SHC-2 displays the highest values: 2.011 ± 0.006 ppm in enamel, 31.089 ± 0.101 ppm in dentine and 32.859 ± 0.665 ppm in cementum. The lowest one is SHC-4 with 0.040 ± 0.001 ppm in enamel and 1.585 ± 0.005 ppm in dentine. The measured ^{234}U/^{238}U activity ratios in dental tissues range from 1.34 to 2.42 and for the ^{230}Th/^{238}U ratio from 1.42 to 2.69 (Table S3). Analytical uncertainties of these isotopic ratios are 0.1%–2.3% (±2σ; Table S3). Plotting these data (Fig. 3) shows that the majority of dental samples fall on the right of ^{230}Th/^{234}U = 1 line excepting SHC-3, for which ^{234}U/^{238}U and ^{230}Th/^{238}U activity ratios in both enamel and dentine are close to 2.0 and 1.9, respectively. For the teeth from Mohui Cave, the ^{234}U/^{238}U activity ratios in enamel (~1.7) are less than those in dentine (~2.0), and the ^{230}Th/^{238}U activity ratios in enamel (~1.8) are also less than those in dentine (~2.3). This type of U–Th isotopic component (*i.e.*, enamel < dentine) are also shown by SHC-4 and SHC-5. For SHC-1 and SHC-2, the ^{234}U/^{238}U activity ratios in dental tissues are relatively close, while the ^{230}Th/^{238}U activity ratios in cementum are apparently higher than those in enamel and dentine.

For Mohui Cave, the MHC-1 and MHC-2 teeth from the layer 3 yielded coupled ESR/U-series age estimates of 1.29 ± 0.11 Ma and

1.69 ± 0.22 Ma, respectively, associated with total dose rates of 1759 ± 187 μGy/y and 1536 ± 218 μGy/y, respectively. For these samples, 55%–85% of the dose rate is contributed by γ-rays from surrounding sediments. The β-dose rates from dentine and sediments then contributed 7%–12% to enamel. The uranium incorporated into the MHC-1 enamel (~1 ppm) results in an internal dose rate accounting for 40% of the total dose rate. The internal dose rate, however, makes up only ~3% of the total for MHC-2, due to the low U-concentration in enamel (<0.1 ppm). U-uptake reconstructions reveal strong U-leaching in MHC-1 dentine, and in both enamel and dentine of MHC-2. For example, the U-concentration in MHC-1 dentine modeled by AU model once reached a value 3 times higher than the present-day (Fig. S1).

Concerning Sanhe Cave, the SHC-1 and SHC-3 teeth from layer 5 produced age estimates of 910 ± 200 ka and 860 ± 180 ka, with an error weighted mean age of 890 ± 130 ka. The SHC-2, SHC-4 and SHC-5 teeth from layer 4 yielded ages of 830 ± 160 ka, 600 ± 150 ka and 760 ± 190 ka, respectively, with an error weighted mean age of 720 ± 90 ka. Given the missing of depths, the uncertainties of sedimentary γ-dose rates were set to 25% to cover a wide and reasonable range, but lead to relatively low precision in ages (20%–25%). The external γ-dose is the main contributor to paleodoses (65%–96%), the β-dose from dentine, cementum and sediment totally produced 3%–15% of the paleodoses, and the internal dose accounts for 10%–20% for SHC-1, SHC-2, SHC-3 teeth, and is <2% for SHC-4 and SHC-5 (Table S5). According to the calculated U-uptake parameters, the dental tissue of SHC-3 experienced nearly linear U-uptake, as shown by the *p*-values of −0.19 for enamel and 0.03 for dentine. All the others, exhibiting activity ratios of $^{230}Th/^{234}U > 1$ and negative *n*-values between −0.002 and −0.001, probably experienced slight U-leaching (Fig. S1).

4. Discussion

4.1. Chronology of the Gigantopithecus fauna at Mohui Cave

The Mohui fauna displays remarkably ancient features, such as the occurrence of *Sinomastodon yangziensis*, *Stegodon huananensis*, *Ailuropoda microta*, *Tapirus sanyuanensis*, *Hespertherium* sp., *C. fengqii*, *S. peii*, *Dorcabune liuchengense* and *H. magna*. These species are typical of the first stage of *Gigantopithecus* fauna, and occur only in the early Pleistocene mammalian assemblages in southern China. The Mohui assemblage closely resembles that at Chuifeng Cave, located 500 m southeast and 12 m higher than Mohui Cave. The two assemblages do not show obvious taxonomic differences. At Chuifeng Cave, the *Gigantopithecus* fauna has been dated between 1.97 ± 0.19 Ma and 1.38 ± 0.17 Ma using coupled ESR/U-series dating and paleomagnetism analysis (Shao et al., 2014b). The new ages from Mohui samples confirm that the two early Pleistocene faunal assemblages are penecontemporaneous (Fig. 4).

The faunal assemblages from Mohui and Chuifeng Caves also resemble the early Pleistocene assemblages at Longgupo (Chongqing) and Liucheng (Guangxi ZAR), which were recently dated by coupled ESR/U-series dating of fossil teeth to 1.4–1.8 Ma (Han et al., 2012) and 0.94–1.21 Ma (Rink et al., 2008). It confirms that the evolutionary stage 1 of *Gigantopithecus* fauna was coeval to the Lower Pleistocene before Jaramillo subchron onset.

4.2. Chronology of the Gigantopithecus fauna at Sanhe Cave

The Sanhe faunal assemblage shows some specificities, suggesting an evolutionary advancement in the *Gigantopithecus* fauna (stage 2) (Table S1). The Sanhe assemblage still contains a number of Neogene mammals, such as *Sinomastodon*, *Dicoryphochoerus* and *Cervavitus*, many extinct Pleistocene genera, including

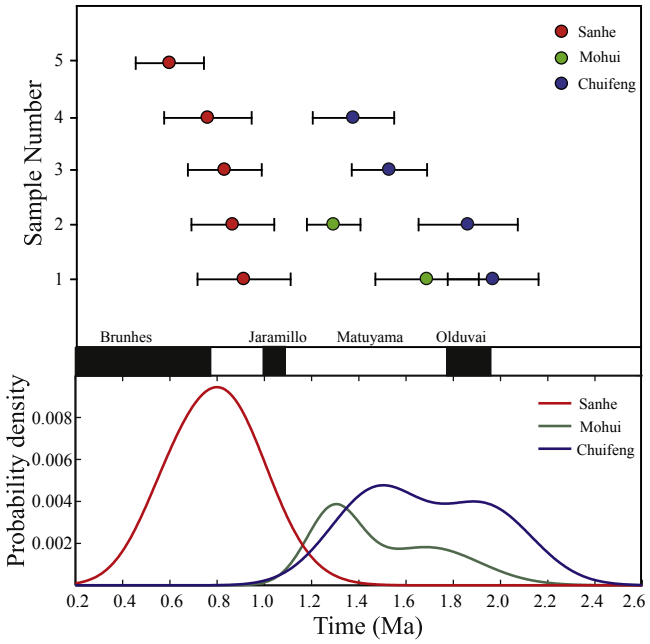

Fig. 4. Coupled ESR/U-series age estimates for *Gigantopithecus* faunas at Sanhe, Mohui, and Chuifeng Caves.

Gigantopithecus, *Procynocephalus*, *Erictis*, *Stegodon*, *Megalovis* and *Bibos*, and many early Pleistocene micromammals, including *Typhlomys intermedius*, *H. magna*, *Belomys parapearsoni*, *Niviventer preconfucianus* and *Leopoldamys edwardsioides*. But the occurrence of relatively advanced species, such as *Ailuropoda wulingshanensis*, *Cuon antiquus* and *Tapirus sinensis*, indicates that the Sanhe fauna is younger than the Mohui and Chuifeng assemblages. Furthermore, the *G. blacki* teeth at Sanhe Cave are significantly larger than those from Mohui and Chuifeng Caves, suggesting that the Sanhe assemblage may be younger (Zhang, 1982).

Paleomagnetism analyses of the Sanhe Cave deposits from 0 to 12 m deep (Sun et al., 2014) identified one segment with reverse polarity, R3, and three with normal polarity, N3–N5 (Fig. 2B). Based on faunal comparisons and paleomagnetic data from the other caves in adjacent areas, the N3, in the lower part of the Sanhe section, was correlated with Olduvai Subchron, and N4 and N5 with Jaramillo Subchron, while R3, containing the *G. blacki*, correlated with pre-Jaramillo Matuyama part (Sun et al., 2014). The age of *Gigantopithecus* fauna in Sanhe Cave was then estimated to be approximately 1.2 Ma (Sun et al., 2014).

The obtained coupled ESR and U-series age estimates suggest that deposition the Sanhe fauna assemblage began in the late early Pleistocene, ~900 ka, and continued into early middle Pleistocene, ~600 ka. According to these radiometric dates, the normal magnetozone N3 of Sun et al. (2014) could be then assigned to the Jaramillo subchron, the normal magnetozones N4 and N5 to the Brunhes chron, and the reverse polarity R3 to the region of Matuyama chron after the Jaramillo subchron.

5. Conclusions

Two teeth from Mohui Cave were dated at 1.69 ± 0.22 Ma and 1.29 ± 0.11 Ma. These ages agree well with those for similar assemblages in Chuifeng Cave, which was recently dated from 1.97 ± 0.19 Ma to 1.38 ± 0.17 Ma (Shao et al., 2014b). For Sanhe Cave, the five samples ranged from 910 ± 200 ka to 600 ± 150 ka. The samples from layers 5 and 4 gave error weighted mean ages of

890 ± 130 ka and 720 ± 90 ka, respectively. Our results suggest that the Sanhe section probably recorded the paleomagnetic transition from the Matuyama to the Brunhes chron. According to these dates, the normal magnetozone (N3) found by Sun et al. (2014) in the lower part of the Sanhe section can be correlated to Jaramillo subchron, the normal magnetozones (N4 and N5) in the upper part of the section can be correlated to Brunhes chron, and the reverse magnetozone (R3), containing the *G. blacki*, can be assigned to the part of Matuyama chron after the Jaramillo subchron. These new results and those from Longgupo and Chuifeng Caves (Han et al., 2012; Shao et al., 2014a,b) suggest that the first two evolution stages of *Gigantopithecus* faunas (Jin et al., 2009, 2014) are penecontemporaneous with the early Pleistocene, between Olduvai and Jaramillo subchrons, and between Jaramillo subchron and B/M boundary, respectively.

Acknowledgments

This study was supported by the National Natural Science Foundation of China (41302136, 41202017) and the Program of China Geological Survey (1212011220519). We thank the EGIDE PHC "Cai Yuanpei" Program (Project 24053YG). We also thank F. Tian and Q.Y. Huang from the Cultural Administration of Tiandong County, Guangxi Autonomous Region for their cooperation with the field work. The authors are grateful to C.-L. Deng for discussions on the results, H. Valladas, E. Pons-Branchu and F. Thil for their help with this project and an anonymous referee for the comments on the manuscript.

Appendix A. Supplementary data

Supplementary data related to this article can be found at http://dx.doi.org/10.1016/j.quageo.2015.04.008.

References

Adamiec, G., Aitken, M., 1998. Dose-rate conversion factors: update. Anc. TL 16, 37–50.
Apers, D., Debuyst, R., De Canniere, P., Dejehet, F., Lombard, E., 1981. A criticism of the dating by electron paramagnetic resonance (ESR) of the stalagmitic floors of the Caune de L'Arago at Tautavel. In: De Lumley, H., Labeyrie, J. (Eds.), Absolute Dating and Isotope Analysis in Prehistory-methods and Limits. CNRS, Paris, pp. 533–550. Prétirage.
Berger, G.W., Huntley, D.J., 1989. Test data for exponential fits. Anc. TL 7, 43–46.
Ciochon, R., Long, V.T., Larick, R., Gonzalez, L., Grün, R., De Vos, J., Yonge, C., Taylor, L., Yoshida, H., Reagan, M., 1996. Dated co-occurrence of *Homo erectus* and *Gigantopithecus* from Tham Khuyen Cave, Vietnam. Proc. Natl. Acad. Sci. U. S. A. 93, 3016–3020.
Ciochon, R.L., Piperno, D.R., Thompson, R.G., 1990. Opal phytoliths found on the teeth of the extinct ape *Gigantopithecus blacki*: implications for paleodietary studies. Proc. Natl. Acad. Sci. U. S. A. 87, 8120–8124.
Driessens, F.C.M., 1980. The mineral in bone, dentine and tooth enamel. Bull. Soc. Chim. Belg. 89, 663–689.
Goldstein, S.J., Stirling, C.H., 2003. Techniques for measuring uranium-series nuclides: 1992–2002. Rev. Miner. Geochem. 52, 23–57.
Grün, R., 2009. The DATA program for the calculation of ESR age estimates on tooth enamel. Quat. Geochronol. 4, 231–232.
Grün, R., Katzenberger-Apel, O., 1994. An alpha irradiator for ESR dating. Anc. TL 12, 35–38.
Grün, R., Schwarcz, H.P., Chadam, J., 1988. ESR dating of tooth enamel: coupled correction for U-uptake and U-series disequilibrium. Nucl. Tracks Radiat. Meas. 14, 237–241.
Han, F., Bahain, J.-J., Boëda, E., Hou, Y., Huang, W., Falguères, C., Rasse, M., Wei, G., Garcia, T., Shao, Q., Yin, G., 2012. Preliminary results of combined ESR/U-series dating of fossil teeth from Longgupo Cave, China. Quat. Geochronol. 10, 436–442.
Huang, W., Ciochon, R., Gu, Y., Larick, R., Fang, Q., Schwarcz, H., Yonge, C., de Vos, J., Rink, W., 1995. Early Homo and associated artefacts from Asia. Nature 378, 275–278.
Jin, C., Wang, Deng, C., Harrison, T., Qin, D., Pan, W., Zhang, Y., Zhu, M., Yan, Y., 2014. Chronological sequence of the early Pleistocene *Gigantopithecus* faunas from cave sites in the Chongzuo, Zuojiang River area, South China. Quat. Int. 354, 4–14.
Jin, C., Qin, D., Pan, W., Tang, Z., Liu, J., Wang, Y., Deng, C., Zhang, Y., Dong, W., Tong, H., 2009. A newly discovered *Gigantopithecus* fauna from Sanhe Cave, Chongzuo, Guangxi, South China. Chin. Sci. Bull. 54, 788–797.
McLean, N.M., Bowring, J.F., Bowring, S.A., 2011. An algorithm for U-Pb isotope dilution data reduction and uncertainty propagation. Geochem. Geophys. Geosyst. 12, Q0AA18. http://dx.doi.org/10.1029/2010GC003478.
Rink, W.J., Wang, W., Bekken, D., Jones, H.L., 2008. Geochronology of *Ailuropoda-Stegodon* fauna and *Gigantopithecus* in Guangxi Province, Southern China. Quat. Res. 69, 377–387.
Shao, Q., Bahain, J.-J., Dolo, J.-M., Falguères, C., 2014a. Monte Carlo simulation of US-ESR age uncertainty. Quat. Geochronol. 22, 99–106.
Shao, Q., Bahain, J.-J., Falguères, C., Dolo, J.-M., Garcia, T., 2012. A new U-uptake model for combined ESR/U-series dating of tooth enamel. Quat. Geochronol. 10, 406–411.
Shao, Q., Bahain, J.-J., Falguères, C., Peretto, C., Arzarello, M., Minelli, A., Hohenstein, U.T., Dolo, J.-M., Garcia, T., Frank, N., Douville, E., 2011. New ESR/U-series data for the early Middle Pleistocene site of Isernia la Pineta, Italy. Radiat. Meas. 46, 847–852.
Shao, Q., Wang, W., Deng, C., Voinchet, P., Lin, M., Zazzo, A., Douville, E., Dolo, J.-M., Falguères, C., Bahain, J.-J., 2014b. ESR, U-series and paleomagnetic dating of *Gigantopithecus* fauna from Chuifeng Cave, Guangxi, Southern China. Quat. Res. 82, 270–280.
Sun, L., Wang, Y., Liu, C., Zuo, T., Ge, J., Zhu, M., Jin, Z., Deng, C., Zhu, R., 2014. Magnetochronological sequence of the early Pleistocene *Gigantopithecus* faunas in Chongzuo, Guangxi, Southern China. Quat. Int. 354, 15–23.
Wagner, G.A., Krbetschek, M., Degering, D., Bahain, J.-J., Shao, Q., Falguères, C., Voinchet, P., Dolo, J.-M., Garcia, T., Rightmire, G.P., 2010. Radiometric dating of the type-site for *Homo heidelbergensis* at Mauer, Germany. Proc. Natl. Acad. Sci. U. S. A. 107, 19726–19730.
Wang, C.-B., Zhao, L., Jin, Z., Wang, Y., Qin, D., Pan, W., 2014a. New discovery of early Pleistocene *Orangutan* fossils from Sanhe Cave in Chongzuo, Guangxi, Southern China. Quat. Int. 354, 68–74.
Wang, W., 2009. New discoveries of *Gigantopithecus blacki* teeth from Chuifeng Cave in the Bubing Basin, Guangxi, South China. J. Hum. Evol. 57, 229–240.
Wang, W., Potts, R., Yuan, B., Huang, W., Cheng, H., Edwards, R.L., Ditchfield, P., 2007. Sequence of mammalian fossils, including hominoid teeth, from the Bubing Basin Caves, South China. J. Hum. Evol. 52, 370–379.
Wang, W., Potts, R., Hou, Y.M., Chen, Y.F., Wu, H.Y., Yuan, B.Y., Huang, W.W., 2005. Early Pleistocene hominid teeth recovered in Mohui Cave in Bubing Basin, Guangxi, South China. Chin. Sci. Bull. 50, 2777–2782.
Wang, Y., Jin, C.Z., Mead, J.I., 2014b. New remains of *Sinomastodon yangziensis* (Proboscidea, Gomphotheriidae) from Sanhe Karst Cave, with discussion on the evolution of Pleistocene *Sinomastodon* in South China. Quat. Int. 339–340, 90–96.
Wang, W., Liao, W., Li, D., Tian, F., 2014c. Early Pleistocene large-mammal fauna associated with *Gigantopithecus* at Mohui Cave, Bubing Basin, South China. Quat. Int. 354, 122–130.
Zhang, Y., 1982. Variability and evolutionary trends in tooth size of *Gigantopithecus blacki*. Am. J. Phys. Anthropol. 59, 21–32.
Zheng, S.H., 2004. Jianshi Hominid Site. Science Press, Beijing, pp. 1–412 (in Chinese).